

Numerical Simulation of Flow past a Circular Cylinder with Varying Tunnel Height to Cylinder Diameter at Re 40.

Rajani B.N¹, R.V.P Gowda² And P. Ranjan²

¹ Computational and Theoretical Fluid Dynamics Department, National Aerospace laboratories, Bangalore 560017, Karnataka, India.

² Dept. of Industrial Engineering, Dayananda Sagar College of Engineering, Shavige Malleshwara Hills, Kumaraswamy layout, Bangalore 560078, Karnataka, India.

Abstract:

The current study mainly focuses on the two-dimensional numerical simulation of the unsteady laminar flow past a circular cylinder in a channel, mimicking the effect of the tunnel wall. The computational results obtained using two different flow solution codes are validated against other computational and measurement data available in the literature. The study confirms a decrease in wake length and a shift in flow separation further downstream at smaller gaps between the tunnel walls and cylinder.

Keywords: Cylinder, OpenFOAM, parabolic flow, tunnel, uniform flow, vortices.

1. Introduction

Flow around a circular cylinder is a challenging kaleidoscopic phenomenon. Cross flow normal to the axis of a circular cylinder and the associated problems of heat and mass transport are encountered in a wide variety of engineering applications. In case of cylinders with regular polygonal cross section, the flow usually separates at one or more sharp corners of the cross-section geometry itself, forming a pair of symmetric vortices in the wake on either side of the mid symmetry plane. On the other hand, for a circular cylinder, where the point of flow separation, decided by the nature of the upstream boundary layer, is not fixed, the physics of the flow is much more complex than its relatively simple shape might suggest. Both experimental measurements and numerical computations have confirmed that beyond a critical Reynolds number the flow structure is attributed mainly to the effect of walls on the flow close to the cylinder. The vortices shed from the wall interact with the vortices shed from the cylinder, hence forming a new vortex structure. Due to close proximity of the tunnel walls, the flow velocity above and below the cylinder increases, resulting in change in pressure field around the cylinder. Experimental studies conducted by Buresti *et al* [1] and Price *et al* [2] also provide a great insight into the change in flow around a cylinder near tunnel walls. However, the experiments conducted in this field of study were at high Reynolds numbers, where flow can no longer be considered two dimensional. Recently, in studies conducted by Sahin *et al* [3], finite volume symmetry is lost and the wake becomes unstable leading to the shedding of alternate vortices from the cylinder surface at a definite frequency, well known in literature as the von Karman vortex street. The size and strength of the symmetric pair of vortex and the Reynolds number at which the onset of the wake instability is observed greatly depends on the blockage effect (ratio of the cylinder diameter to tunnel diameter), cylinder aspect ratio, end plate and any other disturbances arising out of the experimental set up. A brief overview of the flow algorithm employed is presented in Majumdar *et al* [4]. Previously conducted studies, such as Singha *et al* [5] and Zovatto *et al* [6] have shown a significant change in the flow characteristics around a cylinder with close proximity of tunnel walls. In a global point of view, the observation presented in these studies are the same as discussed in this study: A shift in the point of separation downstream and delay in vortex shedding in the proximity of tunnel walls. This change in velocity only formulation was developed in order to study the effects of wall proximity on the flow field around a circular cylinder. Studies of linear stability of the flow were conducted over a range of Reynolds number (0-280) and blockage ratio (0.1-0.9).

Present study emphasizes on two main subjects: understanding the physics of flow around a confined circular cylinder at various values of tunnel height to cylinder diameter aspect ratio (H/D) and understanding the use of OpenFOAM as a solver to solve the defined problem. An in house multiblock structured implicit finite volume flow solution algorithm, 3D PURLES, developed at National Aerospace Laboratories, is used to solve the problem initially. The results are thereafter compared with those obtained from OpenFOAM. The conclusion drawn from the study is thus an effective one, supported by two different flow solution codes. The simulations are carried out long enough for the flow characteristics to evolve. Simulations are carried out at Re 40, consistent with the two-dimensionality assumption. Grids of significantly high resolution are generated using an in-house grid generation tool and a third party software, Gridgen. Emphasis is given to the behavior of wake and the separation length over the surface of the cylinder. Significant changes in wake behavior are seen as the tunnel height is reduced. Reduction in wake length for lower H/D values is seen along with increase in drag on the cylinder. Several important flow characteristics such as separation point and re-circulation length (wake length) in the steady flow regime are correlated with the input parameters (Re and H/D).

2. Problem Statement And Mathematical Formulation.

Numerical simulations of low Reynolds number flow over a circular cylinder placed centrally in a channel with varying height are carried out using a primitive variable based finite volume Navier-Stoke solver, implemented on a structured grid. Figures 1(a) and 1(b) show the schematic diagram of the flow configuration for uniform and parabolic flow profile respectively. The flow simulation is carried out at Re 40, based on the centerline velocity, diameter (D) of the cylinder and normalized tunnel height (H/D). The tunnel height to diameter ratio (H/D) varies in the range: $30 \geq H/D \geq 2$. Based on the study of previous experiments [4,5], the far field boundary is placed initially at $30D$ and grid resolution is fixed at $30 \times 30 \times 1$ to cover the entire domain of the cylinder (azimuthal angle θ varying from 0 to 360 degrees).

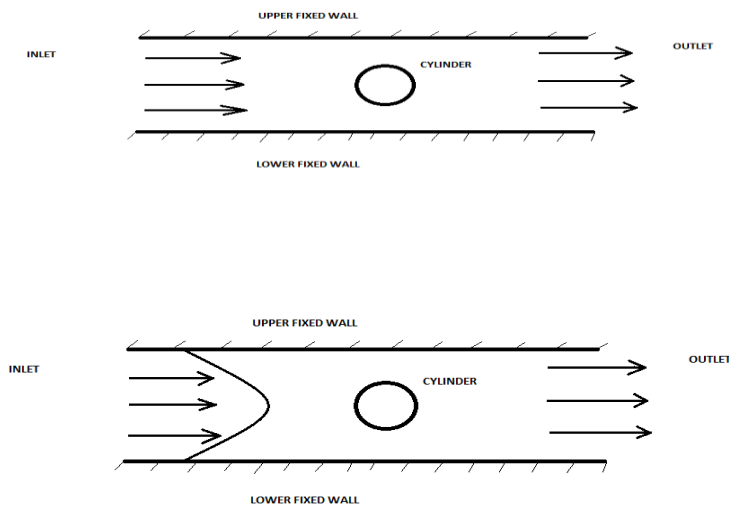


Figure 1: (a) Uniform flow (b) Parabolic flow.

The in house grid generation algorithm involves the solution of the elliptic type differential equations at a coarse level, followed by simple algebraic interpolation from the coarse to a finer level. The coarser grid is primarily generated by solving a system of inverted Poisson equations for a given point distribution at all four boundaries of a two-dimensional computation domain. The control functions in the equations are automatically adjusted in an iterative procedure to achieve boundary-orthogonality and need no ad-hoc adjustment of the problem dependent parameters. Finally, when the desired concentration of grid points is specified at the fine level on one boundary along each direction, the fine level field grid coordinates is obtained by fitting bicubic spline functions passing through the coarse level grid nodes. The Hybrid approach makes a compromise between the simple algebraic and the expensive differential approach and guarantees smooth grid of desired fineness and approximate boundary-orthogonality for a very reasonable computation cost.

The flow computation is carried out using O-topology for the cylinder. Near the cylinder surface, the grid lines are specially stretched along the wall-normal direction in order to have a better resolution of the steep flow variable gradients in the boundary layer. Five different grids are created for previously mentioned cylinder-wall aspect ratios (Table 1). Grid resolution is kept constant for all values of aspect ratios. The grid lines are stretched radially near the cylinder wall to resolve the sharp local gradients of the flow variables.

Table 1: Reynolds numbers and channel heights considered.

Reynolds Number (Re)	40	
Normalized cylinder to wall ratio ($3D - PURLES$)	10,20,30,5 and 2	Uniform and Parabolic
Normalized cylinder to wall ratio (OpenFOAM)	10,20 and 30	Uniform

The numerical solution of the NS equation uses an appropriate mathematical model, which handles the geometrical complexities like arbitrary shaped boundaries as well as the physical complexities like simulating the effect of vortex shedding. In Cartesian coordinates form, the Navier-Stokes equations for a general case are expressed as

$$\frac{\partial(\rho u_i)}{\partial t} + \frac{\partial(\rho u_i u_j)}{\partial x_j} = \frac{\partial(\tau_{ij})}{\partial x_j} + F_i \quad (1)$$

where,

$$\tau_{ij} = -(P + 2/3\mu \frac{\partial u_j}{\partial x_i})\delta_{ij} + 2\mu e_{ij} \quad (2)$$

and

$$e_{ij} = \frac{1}{2} \left(\frac{\partial u_i}{\partial x_j} + \frac{\partial u_j}{\partial x_i} \right) \quad (3)$$

Here $j = 1, 2, 3$ is the summation index of the tensor, τ_{ij} is the stress tensor. δ_{ij} is the Kronecker delta and e_{ij} is the strain rate tensor and μ is the viscosity. With appropriate transformations, the equation is used in 3D-PURLES and OpenFOAM. The equation of continuity becomes

$$\frac{\partial \rho}{\partial t} + \frac{\partial \rho u_i}{\partial x_j} = 0 \quad (4)$$

The governing differential equations for the flow are integrated over a finite number of control volumes covering the computation domain formed by the grid generation procedure. The grid generation procedure calculates the coordinates of the control volume vertices which are simply joined by linear segments to form the six boundary planes and hence the volume. All the variables are stored at the geometric center P of the control volume. The six neighboring control volume centers are denoted by N, S, E, W, T and B for the north, south, east, west, top and bottom neighbors respectively. The face center points n, s, e, w, t and b are located at the intersection of the lines joining the midpoint of the opposite edges, e.g. ne and se are the middle points of the edge forming the east edge with 'e' at its center. These points specified on edges are used for locating the variables and their gradients on the control volume faces. The Cartesian velocities at the control volume faces of control volume are computed and finally the total convective mass fluxes at the cell faces are stored.

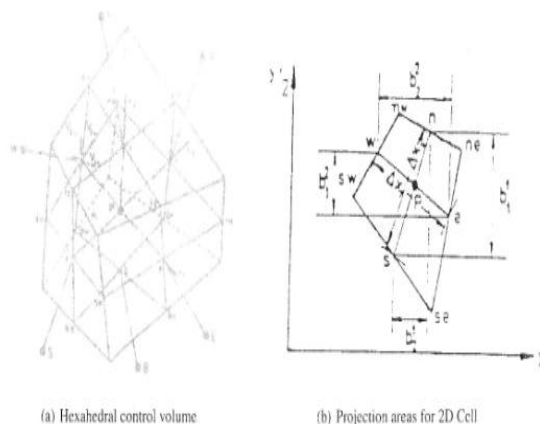


Figure 2: (a) Hexahedral Control volume (b) Projection areas for 2D Cell.

The most important geometrical parameters required in the present formulation are the metric coefficients β_j^i , which may always be expressed in terms of the projection area of the control volume, faces as follows:

$$\beta_i^j = b_j^i \Delta_i / (\Delta x_1 \Delta x_2 \Delta x_3) \quad (5)$$

where the areas b_j^i for the control volume around P are shown in Figure 2(b) for a two dimensional situation on $y_1 - y_2$ plane. The other geometrical quantities of interest are the normal distance of a near boundary node from the boundary surface, the volume and the projection of boundary face areas on the Cartesian reference planes. The calculation of these quantities however involves only some simple arithmetic operations. In addition to the discretised governing equations, the complete specification of the mathematical problem requires the incorporation of proper boundary conditions for all the variables. The appropriate boundary conditions used for the present multiblock computation are shown in Figure 3.

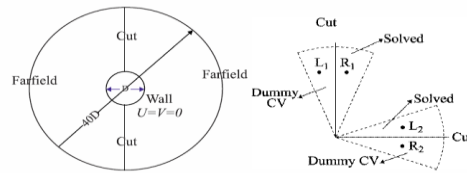


Figure 3: Boundary conditions for a typical two block computation of flow past a cylinder.

The two dimensional flow equations are discretised and solved as follows: Time accurate computations are carried out using the central difference scheme (CDS) for spatial discretization of convective flux coupled to deferred correction procedure (i.e. combining 10% of Upwind fluxes 90% of CDS fluxes) and a second order accurate scheme for temporal discretization. In OpenFOAM, the SimpleFOAM solver is used to solve the problem in steady state conditions. The scheme used is same as that in 3D-PURLES. The convergence criterion (CC) is fixed to be about 10^{-5} for the continuity and momentum equations, for both 3D-PURLES and OpenFOAM.

3. Results.

3.1 Flow at Reynolds number 40: Uniform flow profile.

Simulations are carried out using 3D-PURLES and OpenFOAM with uniform profile ($u_{in}=u_0$) at the inlet as shown in figure 1. The unconfined flow at Re 40 is approaching transition but in the steady, attached wake regime. The bounded flows also belong to the same flow regime. Figures 4 and 5 show the streamlines of the flows for various channel heights. Changes in wake length are observed with the changing tunnel height to cylinder diameter (H/D) ratio. For a smaller value of H/D , the wake is attached to the cylinder and has a shorter length as compared to that for a higher H/D . The kinetic energy of the fluid near the cylinder increases and separation point behind the cylinder moves downstream on the cylinder for a small H/D . Consequently, the normalized wake length (L_w) behind the cylinder becomes smaller. Figure 6 shows the movement of the separation points in terms of the angle measured clockwise from the forward stagnation point as the channel height varies.

According to [5], location of the separation point at Re 45 is analytically given by

$$\theta = 147.3(H/D)^{-0.07}, \quad (6)$$

where, θ is the azimuth angle measured in clockwise direction. The relation holds valid for a lower Reynolds number 40 to a considerable extent. Figure 7 shows the corresponding variation in wake length obtained for the present computation. The length of the wake increases almost linearly up to a certain limit as the channel height varies. In the present simulations, the non-dimensional wake length is observed to increase from about 1.39 and 2.51 at $H/D = 10$ to about 2.30 and 2.62 at $H/D = 30$ in OpenFOAM and 3D PURLES respectively. Significant decrease in the size of the two counter rotating vortices with decrease in H/D is observed in Figures 4 and 5. The wake vortices are strengthened but confined in a short region. The lift and drag coefficients attain constant values quite rapidly after the initial transients settle down. Figure 8 shows lift coefficient remains fixed at zero for all the configurations confirming the symmetric nature of the flows. The vorticity in the flow at different H/D values also shows the symmetric nature of flow. The drag coefficients attain a high value of 2.01 and 1.97 at $H/D = 10$, but significantly reduce to 1.58 and 1.60 at $H/D = 30$, based on the results obtained from 3D PURLES and OpenFOAM respectively.

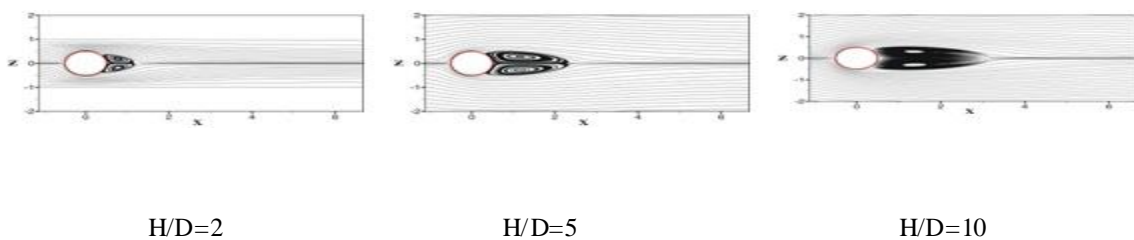




Figure 4: Velocity contours at Re 40 obtained using 3D-PURLES.

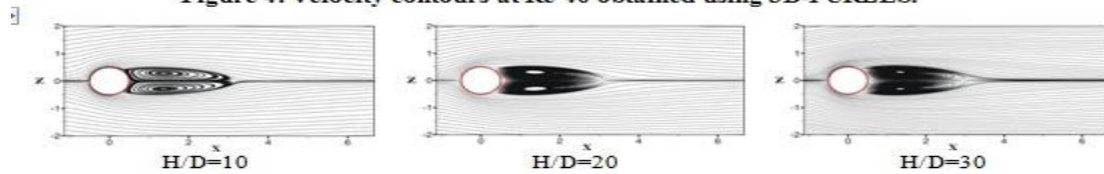


Figure 5: Velocity contours at Re 40 obtained using OpenFOAM.

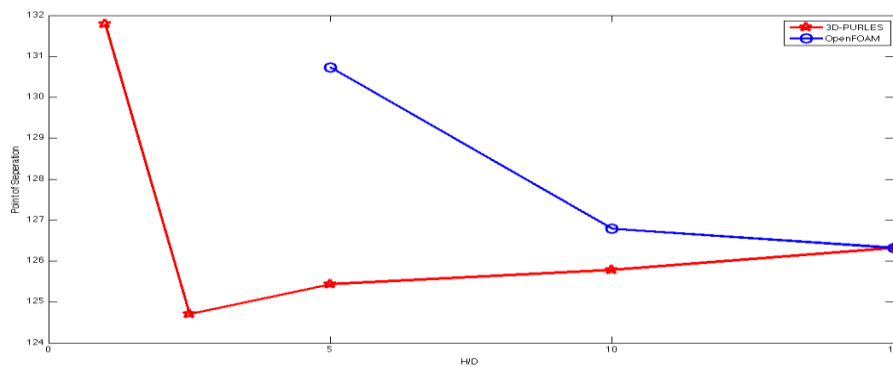


Figure 6: Plot of Point of Separation vs. H/D using 3D PURLES and OpenFOAM.

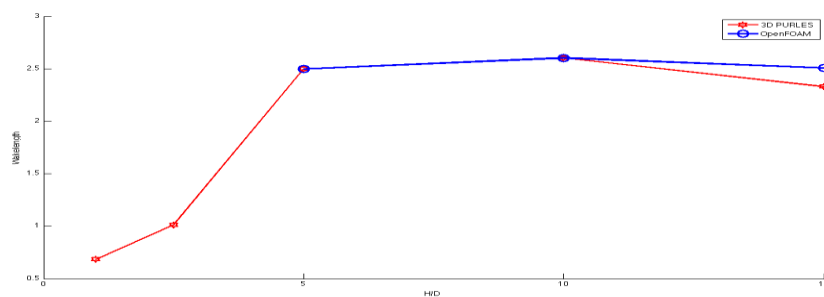


Figure 7: Wake length with H/D; Re = 40 for uniform inlet profile: 3D-PURLES and OpenFOAM.

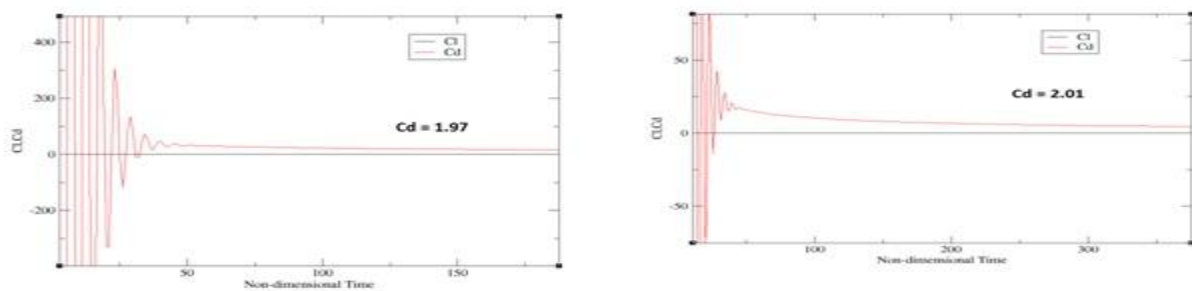


Figure 8: (a) Cl and Cd vs. Non-dimensional time for H/D = 10 at Re 40 using 3D-PURLES.

(b) Cl and Cd vs. Non-dimensional time for H/D = 10 at Re 40 using OpenFOAM.

The vortex strengths in the boundary layers increase and the re-circulation zone attached behind cylinder shortens for H/D up to 8 [5] and then increases for $H/D = 10$ and so on. This causes increased pressure on the front face and a larger drag coefficient at small channel heights. The kinetic energy of the flow decreases with the increase in H/D , causing the boundary layer to shift upstream on the cylinder. The flow separation is observed upstream on the cylinder, causing an increase in wake length.

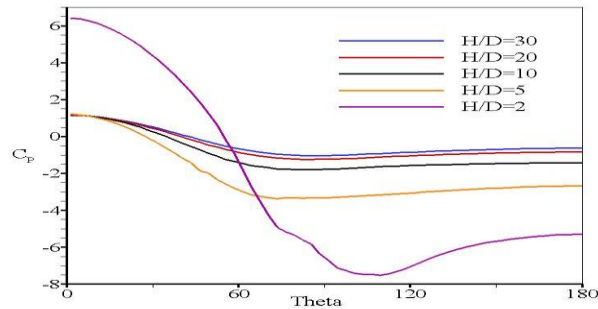


Figure 9: Pressure distribution on the cylinder surface for various channel heights at Re 40 obtained using 3D-PURLES.

The pressure distribution on the cylinder surface for various channel heights is presented in Figure 9, where non-dimensional surface pressure, C_p is plotted against angle measured clockwise from the forward stagnation point. The figure clearly shows considerable increased pressure on the front face when the channel height is small. The pressure falls very fast between $H/D = 30$ and 10 . The results show that the wall proximity effects are most significant for normalized channel height $H/D < 20$. Above this value, the blockage effect on pressure and drag become relatively less effective.

3.2 Flows at Reynolds number 40: Parabolic flow profile.

In the present section, simulations have been carried out with a parabolic flow profile ($u_{in} = u_0[1 - 4(y/H)^2]$) at the inlet as shown in figure 1(b). The observed flow and wake characteristics are different from those of the uniform flow profile to a significant extent. with $H/D = 2$ as the lowest and $H/D = 30$ as the highest. Figure 10 shows the streamlines of the flows for various channel heights using 3D-PURLES. At a low value of $H/D = 2$, the pair of symmetric vortices are compressed and wake length is shorter when compared to the case of uniform flow profile for the same value of H/D . An increase in wake length is observed as the walls move farther away. However the non-dimensional wake length for a parabolic inlet profile is shorter by a significant extent when compared to wake length of uniform flow profile for similar H/D values. The difference between the wake lengths tend to vanish for a value of H/D greater than 10.

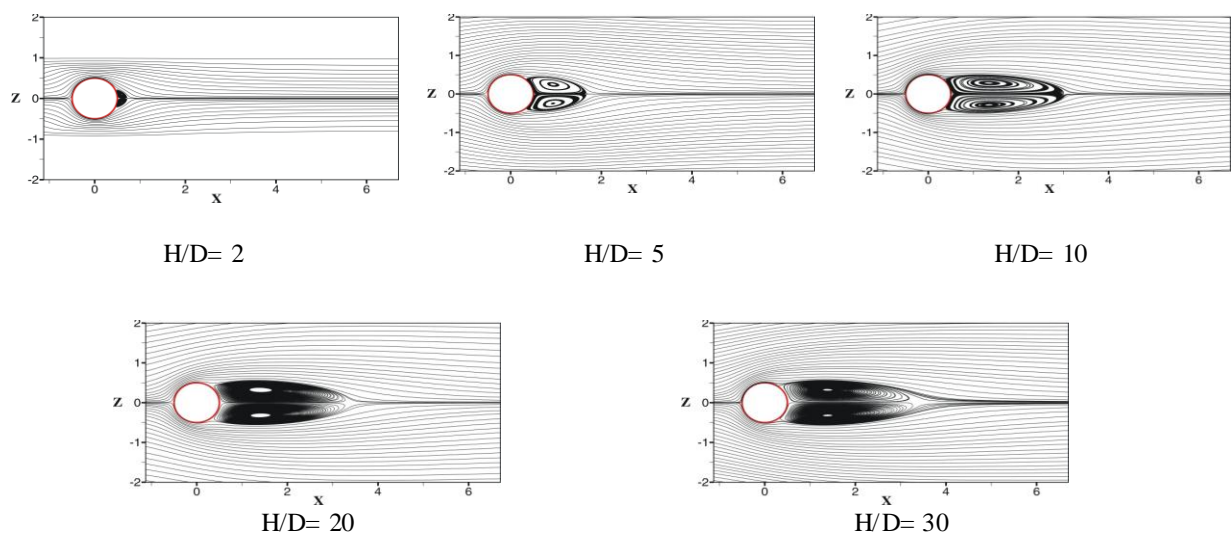


Figure 10: Velocity contours at Re 40 obtained using 3D-PURLES

The pressure distribution on the cylinder surface for various channel heights is presented in Figure 11, where non-dimensional surface pressure, C_p is plotted against angle measured clockwise from the forward stagnation point

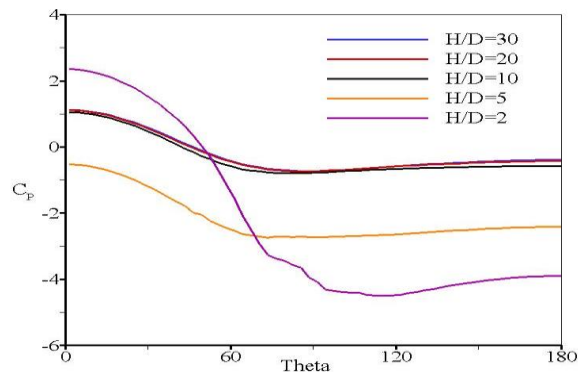


Figure 11: Pressure distribution on the cylinder surface for various channel heights at Re40 obtained using 3D-PURLES.

A short non-dimensional wake length of 0.21 and a high drag coefficient of 2.32 is observed at $H/D = 2$. At a higher value of $H/D = 30$, the flow around the cylinder behaves as an unconfined flow, resulting in an increased wake length of 2.77 and a reduced drag coefficient 1.62. The reasons for such variation between uniform and parabolic flow in terms of wake length and drag coefficient are unknown to the author and need to be investigated.

4. Conclusion

The flow past a circular cylinder symmetrically in a channel is simulated with a primitive variable based second order accurate, structured grid, finite column collocated Navier-Stokes solvers (3D PURLES and OpenFOAM). The cylinder diameter based Reynolds number is 40 with the normalized channel height H/D varying from 10 to 30. Wall proximity is found to have considerable influence on the location of the separation points and length of the closed re-circulating zones in both cases i.e., Uniform flow profile and Parabolic flow profiles. The separation points are found to move rearward resulting in a shorter wake with decreasing channel height only up to a certain limit. Beyond $H/D = 9$, the wake length increases as the walls go farther. The coefficients of drag and lift keep changing based on wall proximity. The value of C_d increases as the walls come closer. Being a steady case and of a non rotating cylinder, the value of C_l is almost zero. The change in the flow structure is mainly attributed to the high energy fluid passing above and below the cylinder due to blockage effect and interacting of tunnel wall vortices with the cylinder vortices. In the end, the computational results obtained from 3D-PURLES and OpenFOAM are comparable to a significant extent.

References

- [1] Buresti, G., Lanciotti, A., Vortex shedding from smooth and roughened cylinders in cross-flow near a plane surface. *The Aeronautical Quarterly* 30(1979), pp305-321.
- [2] Price, S.J., Summer, D., Smith, J.G., Leong, K., Paidoussis, M.P., Flow visualization around a circular cylinder near to a plane wall. In proceedings of the Seventh International Conference on Flow-Induced Vibration., (2000), pp105-114.
- [3] Sahin, M., Owens, R.G., A numerical investigation of wall effects up to high blockage ratios on two-dimensional flow past a confined circular cylinder., 16(2004), pp1305-1320
- [4] Majumdar, S., Pressure based finite volume method for computation of viscous flows, Computational and Theoretical Fluid dynamics Division, National Aerospace Laboratories, Bangalore.
- [5] Singha, S and Sinhamahapatra, K.P, Flow past a circular cylinder between parallel walls at low Reynolds numbers, *J.Ocean engineering*, 37(2010), pp.757-769
- [6] Zovatto, L., Pedrizzetti, G., Flow about a circular cylinder between parallel walls. *Journal of Fluid Mechanics* 440(2001), pp.1-25.